Polyoxometalates

DOI: 10.1002/anie.201004207

Giant Crown-Shaped Polytungstate Formed by Self-Assembly of Ce^{III}-Stabilized Dilacunary Keggin Fragments**

Santiago Reinoso, Mónica Giménez-Marqués, José Ramón Galán-Mascarós, Pablo Vitoria, and Juan M. Gutiérrez-Zorrilla*

Polyoxometalates (POMs) are anionic metal–oxygen clusters with a remarkable variety of structures and potential applications (catalysis, medicine, materials science, and nanotechnology).[1] The combination of their bifunctional activity as H^+/e^- reservoirs with the unique features of 4f ions (luminescence, magnetism, Lewis acid catalysis) is of particular interest and could afford species with enhanced properties owing to synergistic effects. Because of their oxophilicity and high coordination numbers, 4f ions display a powerful ability to link lacunary polytungstates (POTs) to build unprecedented architectures. The larger size of 4f ions compared to 3d metals prevents their full incorporation in lacunary frameworks as addendum atoms, and therefore additional sites are available for further derivatization. For monolacunary POTs, this mainly results in Peacock–Weakley sandwich POTs or in dimers and extended arrangements of 1:1 monomers.[2]

The use of di- and trilacunary building blocks has led to a dramatic increase in the number and size of 4f-containing POTs in recent years. In addition to several medium to large assemblies,[3] this approach has also resulted in a few giant species with more than 100 W atoms,[4] which are amongst the largest POTs known. These are $[As_{12}Ce_{16}W_{148}O_{524}(H_2O)_{36}]^{76-}$,[4a] which has remained the largest POT since 1997; $[Gd_8As_{12}W_{124}O_{432}(H_2O)_{36}]^{60-}$, recently reported as the longest and second-largest POT;[4b] and $[Ce_{20}Ge_{10}W_{100}O_{376}(OH)_4(H_2O)_{30}]^{56-}$, which contains the largest number of 4f ions besides being the fourth-largest POT.[4c] However, these assemblies are still small compared to Mo-blue POMs, for which a cluster as large as Mo_{368} is known.[5] Therefore, the search for giant POTs comparable to Mo blues is an attractive challenge, and supramolecular chemistry of 4f ions and lacunary fragments appears to be a suitable strategy that could allow rational design of tailored assemblies.

Here we report $[K\subset K_7Ce_{24}Ge_{12}W_{120}O_{456}(OH)_{12}(H_2O)_{64}]^{52-}$ (**1**) as the largest tungstogermanate and third-largest POT to date. Besides containing the largest number of 4f ions in a POM, **1** can be considered as the first giant POT with a crown shape, that is, with a ring structure displaying a central cavity available for ion encapsulation in an inorganic analogue of the crown ethers, and thus a new type of topology is added to this still limited family of POMs.

Recently, we reported the first 3d–4f heterometallic POM derived from the Weakley-type structure.[6] With the aim of systematically incorporating 4f ions into this sandwich structure, we replaced half of the 3d precursor by a source of 4f ions in the direct synthesis of Weakley tungstogermanates.[7] Instead of the expected 3d–4f POT, **1** was obtained as $Na_{40}K_6[Ni(H_2O)_6]_3[\mathbf{1}]\cdot n\,H_2O$ (**Ni-1**, $n \approx 178$) in moderate yield from this simple one-pot procedure.

Polyanion **1** (Figure 1 a) can be viewed as the product of the K^+-directed self-assembly of twelve $[Ce_2GeW_{10}O_{38}]^{6-}$ subunits ($\{Ce_2GeW_{10}\}$) formed in situ, each of which is composed of a dilacunary Keggin fragment stabilized by coordination of two Ce ions on the vacant sites through four Ce−O bonds (Figure 1 b). As many as three distinct types of $\{GeW_{10}\}$ skeletons are observed: the enantiomeric forms β(1,8) and β(1,5) and the γ(3,4) fragment,[8] and all of them are of the anti-Lipscomb type.[9] The vacant sites in the β forms are located at the W_3O_{15} group and the central belt, whereas the C_s-symmetric γ(3,4) form is obtained by removal of one WO_6 octahedron from each rotated W_3O_{13} triad (Figure S1, Supporting Information). Among the reported $\{\beta\text{-}XW_{10}\}$-containing POTs,[4c,10] only one β form displays vacancies at the belt and a W_3O_{15} group to the best of our knowledge, namely, β(1,9).[10d] On the other hand, a single γ-dilacunary species was known to date: the C_{2v}-symmetric γ(1,2) form with vacancies at the two edge-sharing octahedra of the rotated triads.[11] Therefore, all three $\{GeW_{10}\}$ fragments in **1** are completely unprecedented and they represent additional, interesting building blocks in POM chemistry.

The fact that $\{Ce_{20}W_{100}\}$, composed of $\{\beta(4,11)\text{-}Ce_2GeW_{10}\}$ subunits, is obtained from the $[A\text{-}\alpha\text{-}GeW_9O_{34}]^{10-}$ precursor at a similar pH[4c] suggests that a diversity of $\{GeW_{10}\}$ isomers may be formed under moderately acidic conditions regardless of the tungstogermanate source. Most likely, they are rapidly interexchangeable, highly reactive intermediates in the formation of the predominant $\{GeW_{11}\}$ species. In both cases, they could be stabilized by Ce coordination, which allowed

---

[*] Dr. S. Reinoso, M. Giménez-Marqués
Instituto de Ciencia Molecular (ICMol)
Universidad de Valencia
Catedrático J. Beltrán 2, 46980 Paterna, Valencia (Spain)
E-mail: santiago.reinoso@uv.es
Dr. J. R. Galán-Mascarós
Catalan Institution for Research and Advanced Studies (ICREA) and Institute of Chemical Research of Catalonia (ICIQ)
Avda. dels Països Catalans 16, 43007 Tarragona (Spain)
P. Vitoria, Prof. J. M. Gutiérrez-Zorrilla
Dpto. Química Inorgánica, Ftad. Ciencia y Tecnología
Universidad del País Vasco (UPV/EHU)
P. O. Box 644, 48080 Bilbao (Spain)

[**] Dr. M. Insausti (UPV/EHU) is gratefully acknowledged for TGA/DTA. BVSumCalc program courtesy of Dr. M. H. Dickman. Financial support by MICINN: grant CTQ2008-03197/BQU and Juan de la Cierva contract (S.R.).

Supporting information for this article is available on the WWW under http://dx.doi.org/10.1002/anie.201004207.

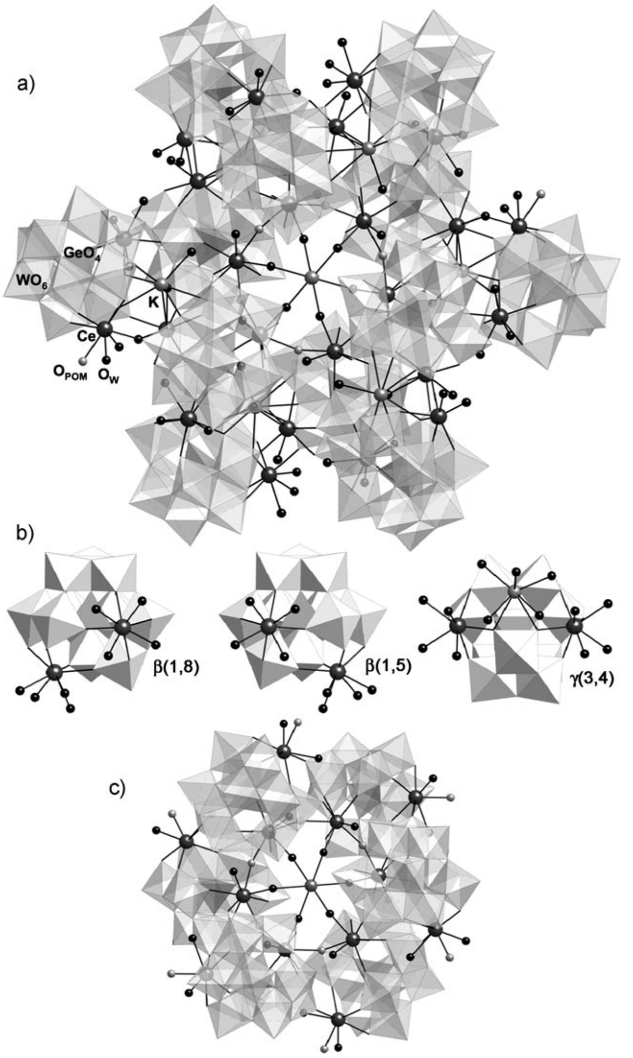

Figure 1. Polyhedral/ball-and-stick representations of a) polyanion **1**; O_W: water. b) β(1,8)-, β(1,5)-, and γ(3,4)-$\{Ce_2GeW_{10}\}$ subunits. c) $K\subset\{\beta\text{-}Ce_2GeW_{10}\}_6$ crown-shaped core.

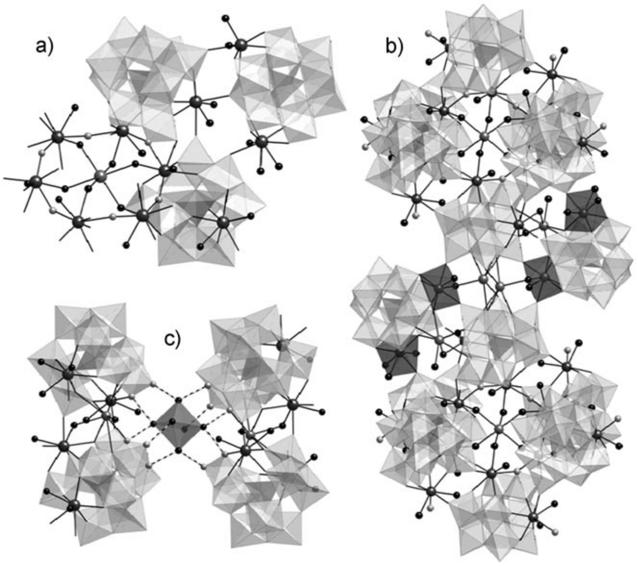

Figure 2. a) $K\subset Ce_6O_{42}$ ring and connectivity between two β- and one γ-$\{Ce_2GeW_{10}\}$ adjacent subunits. b) 1D assembly $[\mathbf{1}]_\infty$ (only the core is depicted; bridging Ce ions represented as square antiprisms). c) $O_{Ni}-H\cdots O_{POM}$ bonding pattern of a $[Ni(H_2O)_6]^{2+}$ cation (dark gray octahedron) buried between two $[\mathbf{1}]_\infty$.

isolation as different POT assemblies. The fact that POTs comprising $\{\beta\text{-}M_2GeW_{10}\}$ subunits[10] are also obtained at pH 4.5–5.5 range starting from $[\gamma\text{-}GeW_{10}O_{36}]^{8-}$ further supports this hypothesis.

Polyanion **1** contains a $[K\subset\{[Ce(H_2O)_2]_2(\beta\text{-}GeW_{10}O_{38})\}_6]^{35-}$ crown-shaped core ($K\subset\{\beta\text{-}Ce_2GeW_{10}\}_6$) composed of three β(1,8)- and three β(1,5)-$\{Ce_2GeW_{10}\}$ subunits arranged alternately (Figure 1 c). Neighboring subunits are linked by coordination of Ce ions in position 1 to two *cis*-related O atoms from the belt WO_6 octahedron adjacent to both vacancies, in such a way that $Ce_1-O_b-Ce_1$ (O_b: bridging oxygen) bridges are formed. This results in a ring of six corner-sharing CeO_8 square-antiprisms in which the Ce atoms are quasicoplanar and display two terminal H_2O molecules, one of which is directed to the inner part of the Ce_6O_6 skeleton (Figure 2 a). This creates a central pocket that hosts a K^+ ion, which therefore shows a six-coordinate geometry best described as distorted octahedral. Although it resembles the crown-shaped $[K\subset\{Eu(H_2O)_2(AsW_9O_{33})\}_6]^{35-}$ to a certain degree,[3e] such a Ce_6O_{42} cyclic motif and subsequent ion capturing by interaction with internal H_2O molecules has not been observed before.

The $K\subset\{\beta\text{-}Ce_2GeW_{10}\}_6$ core displays additional $Ce-O_t-W$ (O_t: terminal oxygen) bridges between belt Ce atoms and corner-sharing CeW_2 groups of $\{\beta\text{-}Ce_2GeW_{10}\}$ neighbors (Figure 2 a). This cyclic arrangement is reinforced by six outer $\{\gamma\text{-}Ce_2GeW_{10}\}$ subunits, connected to two adjacent β subunits through Ce coordination to O_t atoms of the CeW_2 group and the rotated cap, together with Ce–O bonding between the γ-WO_6 octahedron adjacent to both vacancies and belt β-Ce centers. Bond valence sum (BVS) calculations[12] indicate diprotonation of the γ-subunits on the Ce-coordinated O atom of WO_6 positions 9 or 10 (Figure S1, Supporting Information) and on the O_b atom of the W_2O_{10} dimer not linked to K^+ (BVS values: 0.98–1.32). This is fully consistent with elemental analyses.

The assembly of the $\{Ce_2GeW_{10}\}$ subunits results in **1** with C_i symmetry and about 4 nm diameter. The fact that no identifiable products were obtained in the exclusive presence of Na^+ indicates that K^+ plays a key role in the formation of **1**. Thus, K^+ appears to be essential to stabilize the $\{\gamma\text{-}Ce_2GeW_{10}\}$ subunits and their linkage to the crown-shaped core. Moreover, the architecture of **1** suggests that the central K^+ ion acts as an effective template. The geometry of the $\{K(H_2O)_6\}$ fragment imprints the whole architecture, in such a way that **1** can be seen as an arrangement of $\{\gamma\text{-}Ce_2GeW_{10}\}$ subunits with the Ge atoms at the vertices of a highly distorted octahedron, which in turn encloses an analogous octahedron of $\{\beta\text{-}Ce_2GeW_{10}\}$ subunits containing the central $\{K(H_2O)_6\}$ fragment (Figure S2, Supporting Information).

The 24 Ce atoms in **1** display square-antiprismatic geometries with two and three terminal H_2O ligands for β- and γ-Ce atoms, respectively (Figure S3, Supporting Information).

Each polyanion **1** is linked to two neighbors via four γ-Ce–O$_t$–W bridges, resulting in 1D assemblies (Figure 2b) that run along the [010] direction and are arranged in layers parallel to the *ab* plane (Figure S4, Supporting Information). One-third of the $[Ni(H_2O)_6]^{2+}$ cations occupy intralamellar spaces, closely embraced by two β and two γ subunits from adjacent $[\mathbf{1}]_\infty$ chains through 10 strong O_{Ni}–H···O_{POM} hydrogen bonds (Figure 2c). When the one-pot synthetic procedure for **Ni-1** was performed with a source of Co^{2+} or Mn^{2+},[13] the **Co-1** and **Mn-1** analogues were obtained according to the IR spectra (Figure S5, Supporting Information), but using Cu^{2+} led to no identifiable solids. This suggests that the plasticity and Jahn–Teller distortion of Cu^{2+} prevent $[Cu(H_2O)_n]^{2+}$ being buried in the intralamellar cavities, and moreover, that the hydrogen-bonding pattern displayed by regular $[M(H_2O)_6]^{2+}$ octahedral cations is an essential factor for **1** to be isolated.

Due to the similar lengths of all intermolecular Ce–O$_{POM}$ bonds, it is not possible to unambiguously infer from the structure which species could be present in solution after fragmentation of $[\mathbf{1}]_\infty$ chains. To investigate this, a combination of IR, UV/Vis, and dynamic light scattering (DLS) techniques was selected after considering the low solubility and paramagnetism of **Ni-1** as major handicaps for ^{183}W NMR spectroscopy. First, we carried out preliminary IR tests on the stability of the $\{Ce_2GeW_{10}\}$ subunits because the possibility that they undergo transformation to other species could not be disregarded given the unusual structure of the $\{GeW_{10}\}$ fragments. Thus, the IR spectrum of an approximately 2 mM aqueous solution was recorded daily on a single drop placed over a KBr pellet for two weeks. All spectra proved to be virtually identical to that of solid **Ni-1** with no significant shifts or additional peaks, that is, the $\{Ce_2GeW_{10}\}$ subunits remained stable and no other tungstogermanates were formed. Indeed, the solution UV/Vis spectrum also remained unchanged during this time (Figure S6, Supporting Information).

Once the stability of these subunits was confirmed, we monitored the solution by DLS measurements to investigate maintenance of the dodecameric **1** assembly (Figure S7, Supporting Information). Immediately after dissolution, two relatively narrow distributions centered at hydrodynamic diameters of about 2.7 and 195 nm are observed (3:2 relative intensity). Interestingly, the peak at about 2.7 nm splits into two overlapping signals with similar intensities and maxima at about 1.4 and 2.8 nm for an approximately 4 mM solution. These values compare well with the diameters of monomeric $\{Ce_2GeW_{10}\}$ and hexameric K⊂{β-Ce$_2$GeW$_{10}$}$_6$ (ca. 1.1 and 2.5 nm, respectively). The DLS picture is not static: while the peak at about 2.7 nm becomes less intense, the maximum of the second signal shifts to larger diameters and its intensity increases with time, so that it becomes the predominant peak after 48 h. For a six-day-aged solution, the peak at about 2.7 nm cannot be detected anymore, and after two weeks, the second signal is stabilized at about 260 nm, reaching its maximum intensity and narrowest distribution. This behavior resembles that of $[Cu_{20}Cl(OH)_{24}(H_2O)_{12}(P_8W_{48}O_{184})]^{25-}$, which is the smallest POM known to form blackberry-type superstructures in solution and has a size similar to K⊂{β-Ce$_2$GeW$_{10}$}$_6$.[14] These observations show that the dodecameric **1** assembly ($d \approx 4.0$ nm) is not stable on dissolution, and they suggest that the outer {γ-Ce$_2$GeW$_{10}$} subunits are most likely dissociated from the central K⊂{β-Ce$_2$GeW$_{10}$}$_6$ cores. Based on these results, it seems plausible that addition of K^+ to the reaction mixture promotes formation of K⊂{β-Ce$_2$GeW$_{10}$}$_6$ and stabilization of {γ-Ce$_2$GeW$_{10}$}, which assemble together on crystallization with $[Ni(H_2O)_6]^{2+}$ cations. Moreover, the K⊂{β-Ce$_2$GeW$_{10}$}$_6$ hexamers appear to undergo slow self-aggregation to form supramolecular blackberry-type structures. Further investigations on this by static light scattering and microscopy techniques (scanning electron microscopy, atomic force microscopy) are planned and will be reported in due course.

The χT (χ: magnetic susceptibility) product of **Ni-1** at room temperature is in good agreement with that expected for 24 Ce^{III} and three Ni^{II} (20.4 vs. ca. 21 emu K mol^{-1}, Figure S8 in the Supporting Information) and it continuously decreases down to 5 K, where a change in slope and a faster decrease are observed. According to the structure, the Ni^{II} atoms are magnetically isolated and any possible magnetic exchange should come from Ce^{III}–Ce^{III} interactions. Unfortunately, there is a lack of systematic studies on magnetic exchange between paramagnetic 4f ions, so that descriptions of ferro- (F) or antiferromagnetic (AF) weak interactions are scarce.[15] In a related O-bridged hexameric Yb^{III} cluster, magnetic data were fitted by simply taking into account the single-ion anisotropy and a dipolar exchange of only about 0.01 cm^{-1}.[16] Thus, we can assume that only the O-bridged Ce^{III} ions in the Ce_6O_{42} ring could be involved in magnetic exchange, since the O–W–O long pathways between all other Ce^{III} ions would result in negligible interactions.

The high anisotropy of Ce^{III} makes magnetic data very difficult to analyze, because it is responsible for the continuous decrease of χT at high temperature, and prevents observation of Ce^{III}–Ce^{III} interactions in most cases.[17] The $^2F_{5/2}$ free-ion ground sate splits into Kramers doublets because of the ligand field, but strong mixing between ground and excited local Kramers doublets is maintained. Weak magnetic exchange has been claimed only for [Ce$_2$(OAc)$_6$(*o*-phen)$_2$] (*o*-phen = *o*-phenanthroline), in which the presence of a singlet–triplet configuration from the coupling between two "pure" Kramers doublets at very low temperature is assumed.[18] In our case, such an assumption is not feasible because the magnetic moment at low temperature is affected by all magnetically independent Ce^{III} and Ni^{II} ions. Although a quantitative treatment of the data is not possible, we compared the magnetic behavior with that expected for the isolated ions to look for a qualitative analysis (Figure S8, Supporting Information). A good agreement between the two curves is observed at high temperature, but the magnetic moment of **Ni-1** shows a much faster decrease, which suggests the presence of AF interactions. Indeed, an essentially identical Curie constant is found in the $1/\chi$ plot ($C_{exp} = 23.8$, $C_{estim} = 23.0$ emu K mol^{-1}), while the Weiss constant is almost doubled ($\theta_{exp} = -51$, $\theta_{estim} = -30$ K). This feature can only be attributed to the presence of weak AF interactions in the Ce_6O_{42} ring.

In summary, the largest tungstogermanate and third-largest POT, $[K{\subset}K_7Ce_{24}Ge_{12}W_{120}O_{456}(OH)_{12}(H_2O)_{64}]^{52-}$ (**1**), has been obtained in a simple one-pot reaction by K^+-directed self-assembly of three unprecedented types of $\{GeW_{10}\}$ fragments formed in situ and stabilized by coordination of Ce ions on the vacancies. Besides showing the highest number of 4f ions to date, **1** represents the first giant POT with a crown-shaped ring structure. It contains a unique Ce_6O_{42} central ring displaying Ce^{III}–Ce^{III} AF interactions in which a K^+ ion is captured by internal H_2O molecules. Dodecameric **1** most likely dissociates upon dissolution into $\{\gamma\text{-}Ce_2GeW_{10}\}$ monomers and $K\subset\{\beta\text{-}Ce_2GeW_{10}\}_6$ hexamers, which appear to undergo a blackberry-type aggregation that will be studied in the near future. We also plan to systematically investigate the influence of the synthetic variables of this type of one-pot procedure (e.g. solvent, pH, countercation) on the final products.

Experimental Section

Ni-1: Solid $Ce(NO_3)_3\cdot 6H_2O$ (0.426 g, 0.98 mmol), GeO_2 (0.093 g, 0.89 mmol), and $Na_2WO_4\cdot 2H_2O$ (2.640 g, 8.00 mmol) were successively added to a solution of $NiCl_2\cdot 6H_2O$ (0.233 g, 0.98 mmol) in 0.5 M NaOAc/AcOH buffer (40 mL). The reaction mixture was stirred for 1 h. After filtering any solid off, 1 M KCl (0.5 mL) was added to the resulting yellow solution. Single crystals suitable for X-ray diffraction were obtained by slow evaporation at room temperature after about 4 d (0.65 g, 24 %). Elemental analysis (%) calcd for $Ce_{24}Ge_{12}H_{532}K_{14}Na_{40}Ni_3O_{716}W_{120}$: Ce 8.42, Ge 2.18, K 1.37, Na 2.30, Ni 0.44, W 55.25; found: Ce 8.42, Ge 2.27, K 1.39, Na 2.24, Ni 0.40, W 54.24; IR: $\tilde{\nu} = 941$ (s), 824 (vs), 785 (vs), 700 (s), 488 (w), 457 (w), 430 cm^{-1} (w). TGA/DTA: 11.7 % mass loss due to endothermic release of about 260 H_2O molecules below 225 °C (Figure S10, Supporting Information), of which 218 were determined by X-ray diffraction. Two exothermic peaks in the range 510–570 °C indicate final decomposition.

Crystal data for **Ni-1**: $Ce_{24}Ge_{12}H_{532}K_{14}Na_{40}Ni_3O_{716}W_{120}$, $FW = 39931.3\ g\,mol^{-1}$, triclinic $P\bar{1}$, $a = 25.123(2)$, $b = 27.424(3)$, $c = 30.816(3)$ Å, $\alpha = 75.387(3)$, $\beta = 73.270(3)$, $\gamma = 69.846(4)°$, $V = 18809(3)$ Å^3, $T = 100(2)$ K, $Z = 1$, $\rho_{calcd} = 3.525\ g\,cm^{-3}$, $\mu = 20.435\ mm^{-1}$, $2\theta_{max} = 52.0°$, 201 910 reflections, 69 657 unique ($R_{int} = 0.089$), 43 862 observed ($I > 2\sigma I$), 2130 parameters, $R(F) = 0.076$ ($I > 2\sigma I$), $wR(F)^2 = 0.233$ (all data), GoF = 1.035, max./min. electron densities 6.408/−4.553 e Å^{-3}, orange plate ($0.01 \times 0.10 \times 0.20\ mm^3$). Bruker-Nonius Kappa APEX II (4 K CCD detector, monochromated $Mo_{K\alpha}$ radiation, $\lambda = 0.71073$ Å). Further details on the crystal structure investigations may be obtained from the Fachinformationszentrum Karlsruhe, 76344 Eggenstein-Leopoldshafen, Germany (fax: (+49) 7247-808-666; e-mail: crysdata@fiz-karlsruhe.de), on quoting the depository number CSD-380477.

Received: July 9, 2010
Published online: September 22, 2010

Keywords: cerium · magnetic properties · polyoxometalates · self-assembly · supramolecular chemistry

---

[1] a) M. T. Pope, *Heteropoly and Isopoly Oxometalates*, Springer, Berlin, **1983**; b) M. T. Pope, A. Müller, *Angew. Chem.* **1991**, *103*, 56; *Angew. Chem. Int. Ed. Engl.* **1991**, *30*, 34; c) *Polyoxometalates: From Platonic Solids to Antiretroviral Activity* (Eds.: M. T. Pope, A. Müller), Kluwer, Dordrecht, **1994**; d) *Polyoxometalate Chemistry: From Topology via self-Assembly to Applications* (Eds.: M. T. Pope, A. Müller), Kluwer, Dordrecht, **2001**; e) *Polyoxometalate Chemistry for Nanocomposite Design* (Eds.: M. T. Pope, T. Yamase), Kluwer, Dordrecht, **2002**; f) *Polyoxometalate Molecular Science* (Eds.: J. J. Borrás-Almenar, E. Coronado, A. Müller, M. T. Pope), Kluwer, Dordrecht, **2003**; g) M. T. Pope in *Comprehensive Coordination Chemistry II* (Eds.: J. A. McCleverty, T. J. Meyer), Elsevier, Oxford, **2004**.

[2] See, for example: a) B. S. Bassil, M. H. Dickman, B. von der Kammer, U. Kortz, *Inorg. Chem.* **2007**, *46*, 2452; b) M. Sadakane, A. Ostuni, M. T. Pope, *J. Chem. Soc. Dalton Trans.* **2002**, 63; c) M. Sadakane, M. H. Dickman, M. T. Pope, *Angew. Chem.* **2000**, *112*, 3036; *Angew. Chem. Int. Ed.* **2000**, *39*, 2914.

[3] a) F. L. Sousa, F. A. Almeida Paz, A. M. V. Cavaleiro, J. Klinowski, H. I. S. Nogueira, *Chem. Commun.* **2004**, 2656; b) G. Xue, J. Vaissermann, P. Gouzerh, *J. Cluster Sci.* **2002**, *13*, 409; c) W. Chen, Y. Li, Y. Wang, E. Wang, Z. Su, *Dalton Trans.* **2007**, 4293; d) R. C. Howell, F. G. Perez, S. Jain, W. DeW. Horrocks, Jr., A. L. Rheingold, L. C. Francesconi, *Angew. Chem.* **2001**, *113*, 4155; *Angew. Chem. Int. Ed.* **2001**, *40*, 4031; e) K. Fukaya, T. Yamase, *Angew. Chem.* **2003**, *115*, 678; *Angew. Chem. Int. Ed.* **2003**, *42*, 654; f) F. Hussain, B. Spingler, F. Conrad, M. Speldrich, P. Kögerler, C. Boskovic, G. R. Patzke, *Dalton Trans.* **2009**, 4423; g) D. Drewes, M. Piepenbrink, B. Krebs, *Z. Anorg. Allg. Chem.* **2006**, *632*, 534; h) F. Hussain, R. W. Gable, M. Speldrich, P. Kögerler, C. Boskovic, *Chem. Commun.* **2009**, 328.

[4] a) K. Wassermann, M. H. Dickman, M. T. Pope, *Angew. Chem.* **1997**, *109*, 1513; *Angew. Chem. Int. Ed. Engl.* **1997**, *36*, 1445; b) F. Hussain, F. Conrad, G. R. Patzke, *Angew. Chem.* **2009**, *121*, 9252; *Angew. Chem. Int. Ed.* **2009**, *48*, 9088; c) B. S. Bassil, M. H. Dickman, I. Römer, B. von der Kammer, U. Kortz, *Angew. Chem.* **2007**, *119*, 6305; *Angew. Chem. Int. Ed.* **2007**, *46*, 6192.

[5] A. Müller, E. Beckmann, H. Bögge, M. Schmidtmann, A. Dress, *Angew. Chem.* **2002**, *114*, 1210; *Angew. Chem. Int. Ed.* **2002**, *41*, 1162.

[6] S. Reinoso, J. R. Galán-Mascarós, *Inorg. Chem.* **2010**, *49*, 377.

[7] U. Kortz, S. Nellutla, A. C. Stowe, N. S. Dalal, Y. Rauwald, W. Danquah, D. Ravot, *Inorg. Chem.* **2004**, *43*, 2308.

[8] The numbering refers to the positions of the lost WO_6 octahedra. The lowest numeral possible has been assigned to the vacant sites. For the IUPAC nomenclature, see: Y. P. Jeannin, *Chem. Rev.* **1998**, *98*, 51.

[9] W. N. Lipscomb, *Inorg. Chem.* **1965**, *4*, 132.

[10] a) U. Kortz, Y. P. Jeannin, A. Tézé, G. Hervé, S. Isber, *Inorg. Chem.* **1999**, *38*, 3670; b) F. Hussain, B. S. Bassil, L.-H. Bi, M. Reicke, U. Kortz, *Angew. Chem.* **2004**, *116*, 3567; *Angew. Chem. Int. Ed.* **2004**, *43*, 3485; c) B. Botar, Y. V. Geletii, P. Kögerler, D. G. Musaev, K. Morokuma, I. A. Weinstock, C. L. Hill, *Dalton Trans.* **2005**, 2017; d) B. S. Bassil, M. H. Dickman, U. Kortz, *Inorg. Chem.* **2006**, *45*, 2394; e) Z. Zhang, Y. Li, E. Wang, X. Wang, C. Qin, H. An, *Inorg. Chem.* **2006**, *45*, 4313; f) N. H. Nsouli, S. S. Mal, M. H. Dickman, U. Kortz, B. Keita, L. Nadjo, J. M. Clemente-Juan, *Inorg. Chem.* **2007**, *46*, 8763; g) B. Botar, P. Kögerler, *Dalton Trans.* **2008**, 3150; h) N. H. Nsouli, M. Prinz, M. Damnik, M. Neumann, E. Talik, U. Kortz, *Eur. J. Inorg. Chem.* **2009**, 5096; i) B. Botar, A. Ellern, P. Kögerler, *Dalton Trans.* **2009**, 5606.

[11] a) J. Canny, A. Tézé, R. Thouvenot, G. Hervé, *Inorg. Chem.* **1986**, *25*, 2114; b) W. H. Knoth, R. L. Harlow, *J. Am. Chem. Soc.* **1981**, *103*, 1865; c) N. H. Nsouli, B. S. Bassil, M. H. Dickman, U. Kortz, B. Keita, L. Nadjo, *Inorg. Chem.* **2006**, *45*, 3858.

[12] I. D. Brown, D. Altermatt, *Acta Crystallogr. Sect. B* **1985**, *41*, 244.

[13] **Co-1** and **Mn-1** were synthesized as described for **Ni-1**, but by using 0.98 mmol of $CoCl_2\cdot 6H_2O$ (0.233 g) or $MnCl_2\cdot 4H_2O$ (0.194 g).

[14] G. Liu, T. Liu, S. S. Mal, U. Kortz, *J. Am. Chem. Soc.* **2006**, *128*, 10103.

[15] a) J.-P. Costes, J. M. Clemente-Juan, F. Dahan, F. Nicodème, M. Verelst, *Angew. Chem.* **2002**, *114*, 333; *Angew. Chem. Int. Ed.*

2002, *41*, 323; b) H. Hou, G. Li, L. Li, Y. Zhu, X. Meng, Y. Fan, *Inorg. Chem.* **2003**, *42*, 428; c) A. M. Atria, R. Baggio, M. T. Garland, J. C. Muñoz, O. Peña, *Inorg. Chim. Acta* **2004**, *357*, 1997; d) G. Novitchi, S. Shova, J.-P. Costes, O. Mamula, M. Gdaniec, *Inorg. Chim. Acta* **2005**, *358*, 4437; e) R. Baggio, R. Calvo, M. T. Garland, J. C. Muñoz, O. Peña, M. Perec, A. Rizzi, *Inorg. Chem.* **2005**, *44*, 8979; f) D. John, W. Urland, *Eur. J. Inorg. Chem.* **2005**, 4486; g) S. V. Eliseeva, M. Ryazanov, F. Gumy, S. I. Troyanov, L. S. Lepnev, J.-C. G. Bünzli, N. P. Kuzmina, *Eur. J. Inorg. Chem.* **2006**, 4809; h) S.-S. Bao, L.-F. Ma, Y. Wang, L. Fang, C.-J. Zhu, Y.-Z. Li, L.-M. Zheng, *Chem. Eur. J.* **2007**, *13*, 2333.

[16] X. Fang, T. M. Anderson, C. Benelli, C. L. Hill, *Chem. Eur. J.* **2005**, *11*, 712.

[17] G. Abbas, Y. Lan, G. Kostakis, C. E. Anson, A. K. Powell, *Inorg. Chim. Acta* **2008**, *361*, 3494.

[18] A. Panagiotopoulos, T. F. Zafiropoulos, S. P. Perlepes, E. Bakalbassis, I. Masson-Ramade, O. Kahn, A. Terzis, C. P. Raptopoulou, *Inorg. Chem.* **1995**, *34*, 4918.